

# Surface Acoustic Wave (SAW) Tactile Display Based on Properties of Mechanoreceptors

Takaaki NARA, Masaya TAKASAKI, Taro MAEDA,  
Toshiro HIGUCHI, Shigeru ANDO, and Susumu TACHI  
Graduate School of Engineering  
The University of Tokyo  
Bunkyo-ku, Tokyo  
nara@alab.t.u-tokyo.ac.jp

## Abstract

*In this paper, we first analyze dynamic properties of rapidly adapting mechanoreceptors in order to derive a principle of tactile displays. It is shown that Meissner corpuscles with coiled axons and Pacinian corpuscles with layered lamellae are suited to detect equivoluminal distortion of a skin. Combining these analyses with a model of a contact and a relative motion between an object and the skin, it is shown that a prerequisite for tactile displays is to generate sources of shear stress that can be spatially dispersed at the skin surface and temporally modulated with a stick-slip frequency determined by parameters of the object to be displayed. As a device that satisfies this prerequisite, we propose a tactile display using Surface Acoustic Waves (SAW). The roughness of the surface can be changed continuously by controlling the burst frequency of the SAW.*

## 1 Introduction

Development of realistic tactile displays has been a great challenge in Virtual Reality. Varied actuators such as miniature loudspeakers[1], a single micropin[2], a pin array[3], pneumatic actuators[4], and ultrasonic vibrators[5] have been used for displays.

Methods based on the processing properties of human tactile information have also been proposed. Tactile sensations are generated by activation of mechanoreceptive units that are classified into four categories, namely rapidly adapting I and II (RAI, RAI) and slowly adapting I, II (SAI, SAII), whose end organs are Meissner corpuscles, Pacinian corpuscles, Merkel cell-neurite complexes, and Ruffini endings, respectively[6]. Shinoda developed a tactile display that stimulates each mechanoreceptor selectively, using an elastic transfer property of a skin[7]. Kajimoto conducted electrical selective stimulation to the receptors[8].

However, because parameters that characterize roughness, rigidity, and material quality for general objects were not clarified in detail, a principle for displaying general objects by the above devices was not shown, which resulted in using *ad hoc* stimulation in the displays for creating particular sensations.

Furthermore, the mechanisms for the motion of the mechanoreceptors have not been considered at all. Clarifying mechanical properties of the receptors should enable us to obtain a more effective method for stimulating the processing system of human tactile sensation.

Thus, in this paper, we first derive models of Meissner and Pacinian corpuscles that play an important role in active touch. In section 2 we analyze what they detect inside the skin. In section 3, we express dominant skin deformation detected by the receptors in terms of the specific parameters of objects. By combining these analyses, a flow of tactile information from the parameters of objects to the deformation of the receptors is specified. This flow leads to the creation of a principle that shows effective stimulation for tactile control. Based on this principle, we propose a novel tactile display using SAW in section 4.

## 2 Models of mechanoreceptors

### 2.1 Meissner corpuscles

Meissner corpuscles, which have a relatively low characteristic frequency of about 40[Hz], are localized in the papillary dermis with a height of around 150[ $\mu\text{m}$ ] and a diameter of 40~70[ $\mu\text{m}$ ]. A structural feature is their coiled axons[9] on which  $\text{Ca}^{2+}$  ion channels exist[10]. It is known[1] that an open probability of general mechanosensitive ion channels depends on energy of deformation expressed as  $U = K/2 \cdot (\Delta A/A)^2 \cdot A$ , where  $K$  is an elastic modulus of the channel and  $A$  is the size of the channel. Thus,

it is necessary to analyze deformation of the axon surface when stress by skin is applied to the corpuscles. We discuss below the role of coiled axons of Meissner corpuscles for detecting mechanical deformation of the skin.

### 2.1.1 Transmission of deformation by a coil

We first clarify mechanical properties of a coiled structure. As shown in Fig.1, we set an  $x$  axis along the line of the coil and  $y, z$  axes in a section of the line. When normal (Fig.1a) and shear (Fig.2a) stresses are applied to the coil, a torsional moment of  $M_x$  and bending moments of  $M_y, M_z$ . It is noteworthy that only the torsional moment is generated when  $P$  is applied to the coil. As a result, only shear deformation is generated on a coil surface when normal stress is applied to the coil (Fig.1b), while stretch deformation, in addition to shear deformation, is created on the surface when shear stress is applied to the coil (Fig.2b)).

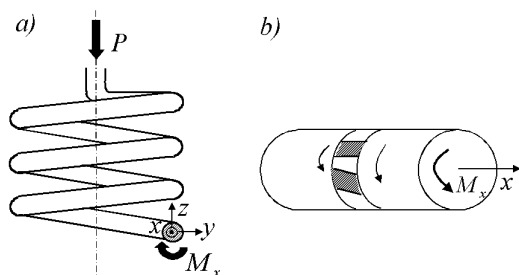


Figure 1: When vertical stress is applied to the coil, a) a torsional moment  $M_x$  is generated at a cross section of the line, b) which results in the creation of a shearing deformation at the line's surface

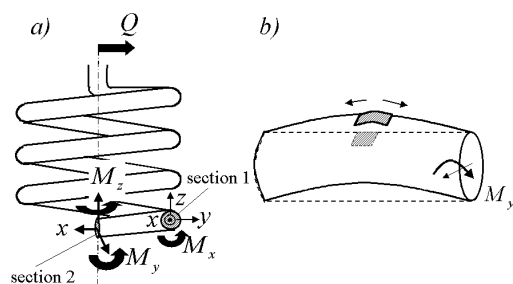


Figure 2: When shear stress is applied to the coil, a) in addition to a torsional moment  $M_x$ , bending moments  $M_y, M_z$  are generated at cross sections of the line, b) which results in the creation of shearing and stretch deformations at the line's surface

Considering that activation of the axon depends on the ratio of change of the channel size, only the shear stress to the coil, which generates stretch deformations on the coil surface, changes the size of the surface so as

to increase the open probability of the channel. Therefore, a hypothesis that the coiled axon of Meissner corpuscles detects shear stress in the skin is derived. For a verification of the statement, we show next that a tuning curve of the corpuscles can be derived on the basis of the shearing resonant character of the coiled axon.

### 2.1.2 Dynamic properties of a coil

A coil's longitudinal resonant frequency of  $\omega_z$  and a shearing resonant frequency of  $\omega_x$  are expressed as

$$\omega_z = \frac{d}{nD^2} \sqrt{\frac{\mu}{2\rho}}, \quad \frac{\omega_x}{\omega_z} = \sqrt{\frac{2(1+\nu)}{1+12(2+\nu)\left(\frac{H}{D}\right)^2}}, \quad (1)$$

where  $d$ : the diameter of the line of the coil,  $\mu$ : the rigidity of the line,  $\rho$ : the density of the line,  $\nu$ : the Poisson's ratio of the line. Assuming that  $\nu \sim 0.5$  and  $H/D = 150[\mu\text{m}]/50[\mu\text{m}]$  as in the Meissner corpuscles,

$$\frac{\omega_x}{\omega_z} = \frac{1}{10}. \quad (2)$$

Thus, it is supposed that the characteristic frequency of the corpuscles derives from the shearing resonant frequency as the minimum resonant frequency of the coiled axon. In fact, with parameters observed in medical experiments [12],  $\omega_x/2\pi = 44[\text{Hz}]$  which corresponds to the real characteristic frequency. Moreover, the tuning curve itself can be driven from the energy of the shearing deformation of the coil, which depends on the shear stress in the skin, as shown in Fig.3. In this way, it is hypothesized that Meissner corpuscles might easily detect shearing, equivoluminal deformation in the skin.

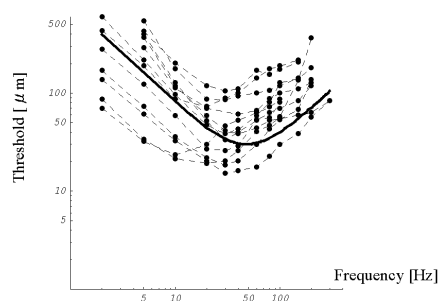


Figure 3: The tuning curve of the Meissner corpuscles: - - -: experiment [13] —: theory Assuming that the Meissner corpuscles detect shear stress of the skin, the tuning curve can be driven from the shearing resonant characteristic of the coiled axon

## 2.2 Pacinian corpuscles

We next consider another RA-type mechanoreceptor, the Pacinian corpuscle. The structure of the corpuscle is that an inner core including an axon is surrounded by concentric 20~70-ply layered lamellae as the section is schematically drawn in Fig.4. Neighboring lamellae are connected by collagen fibers. Gaps between the neighboring lamellae are filled with liquid[14].

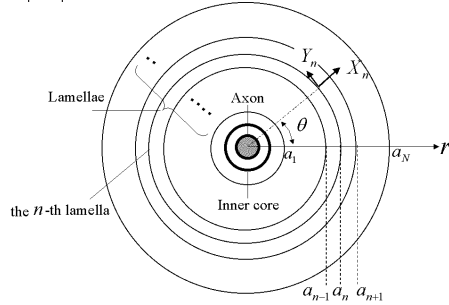


Figure 4: A schematic description of a section of a Pacinian corpuscle

Although models of Pacinian corpuscles are proposed by Loewenstein[15] and Bell[16], only the simplest deformation (Fig.5;  $m=2$ ), or a certain specific deformation, is given to the outermost lamella as a boundary condition for a correspondence to physiological experiments[17].

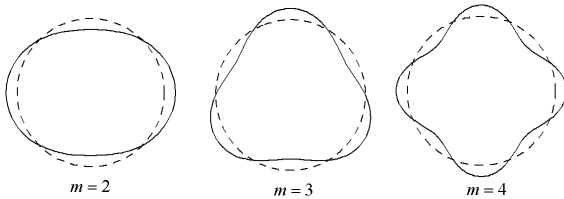


Figure 5: 'Modes' of deformations of Pacinian corpuscles: Arbitrary deformation applied to the corpuscle inside the skin is represented as a summation of modes

To consider arbitrary deformations inside the skin, we express displacements and external forces in the  $\theta, r$  directions of the  $n$ -th lamella at  $r = a_n$  by a summation of the  $m$ -th order mode (Fig.5) expressed as

$$Y_n = Y_{n,m} \cdot \sin m\theta, \quad X_n = X_{n,m} \cdot \cos m\theta \quad (3)$$

$$p_\theta = (F_{n,m} + T_{n,m}) \sin m\theta, \quad p_r = (F_{n,m} + S_{n,m}) \cos m\theta, \quad (4)$$

where  $F_{n,m}$ : an elastic force by collagen fibers, and  $T_{n,m}, S_{n,m}$ : shear and normal stresses by liquid. An isotropic stretch represented by  $m = 0$  is excluded because the corpuscles contain incompressible liquid. A parallel movement of  $m = 1$  is also excluded here. On

the assumption that a lamella is a cylindrical shell, by substituting (3), (4) into Donnell's equations as

$$\frac{C}{a_n^2} \left( \frac{\partial^2 Y_n}{\partial \theta^2} + \frac{\partial X_n}{\partial \theta} \right) + p_\theta = 0, \quad (5)$$

$$-\frac{D}{a_n^4} \frac{\partial^4 X_n}{\partial \theta^4} - \frac{C}{a_n^2} \left( \frac{\partial Y_n}{\partial \theta} + X_n \right) + p_r - M \frac{\partial^2 X_n}{\partial t^2} = 0, \quad (6)$$

we obtain an equation about the displacement of  $X_{n,m}$  in the  $r$  direction as

$$M \ddot{X}_{n,m} = -k_n X_{n,m} + \frac{m-1}{m} F_{n,m} + \left( S_{n,m} - \frac{1}{m} T_{n,m} \right), \quad (7)$$

where  $\rho$ : the density of the shell,  $t$ : the thickness of the shell,  $M = \rho d$ ,  $C = Ed/(1-\nu^2)$ : the shell's rigidity of stretch,  $D = Ed^3/12(1-\nu^2)$ : the shell's rigidity of bending, and  $k_n = m^4 D/a_n^4$  is a shell's equivalent spring constant. Here, it can be shown that the elastic force by collagen fibers is expressed as

$$F_{n,m} = G_{n+1}(X_{n+1,m} - X_{n,m}) - G_n(X_{n,m} - X_{n-1,m}), \quad (8)$$

and the force by viscosity of liquid is represented as

$$S_{n,m} - \frac{1}{m} T_{n,m} = -R_{n,m}(\alpha_m \dot{X}_{n+1,m} - 2\dot{X}_{n,m} + \beta_m \dot{X}_{n-1,m}),$$

$$\text{where } R_{n,m} = \frac{2\mu}{a_n} \cdot \frac{m^2 - 1}{m}.$$

$$\frac{\gamma^{4m} + m\gamma^{2m+2} - m\gamma^{2m-2} - 1}{\gamma^{4m} - m^2\gamma^{2m+2} + 2(m^2 - 1)\gamma^{2m} - m^2\gamma^{2m-2} + 1},$$

$$\alpha_m = 2\gamma^{m+1} \cdot \frac{(m+1)\gamma^{2m} - m\gamma^{2m-2} - 1}{\gamma^{4m} + m\gamma^{2m+2} - m\gamma^{2m-2} - 1},$$

$$\beta_m = 2\gamma^{m-1} \cdot \frac{\gamma^{2m} + m\gamma^2 - (m+1)}{\gamma^{4m} + m\gamma^{2m+2} - m\gamma^{2m-2} - 1}, \quad (9)$$

$\mu$ : viscosity, and  $\gamma = a_{n+1}/a_n$ . Thus, by solving simultaneous equations of (7) for  $n = 1..N$  ( $n = 1$ : the innermost lamella,  $n = N$ : the outermost lamella), lamellae's amplitudes in a sinusoidal vibration can be obtained. Fig. 6 depicts a relation between the order of the mode and an amplitude of the innermost lamella with a frequency of 100[Hz]. It can be seen that the amplitude of only the mode of  $m = 2$  reaches the inner core.

This model is verified by a derivation of a tuning curve of Pacinian corpuscles (Fig.7) in the mode of  $m = 2$  according to the physiological experiment[17]. Parameters used here [14][15] are  $\rho = 10^3$ [kg/m<sup>3</sup>],  $\mu = 0.6 \times 10^{-3}$ [Ns/m<sup>2</sup>] (40 !n),  $N = 40$ ,  $E = 5 \times 10^5$ [N/m<sup>2</sup>],  $d = 1$ [ $\mu$ m],  $a_0 = 10$ [ $\mu$ m], and  $\gamma = 1.083$ . Because it is indicated that a mechanical filter by lamellae contributes to the tuning curve below the characteristic frequency[16], validity of the model that coincides

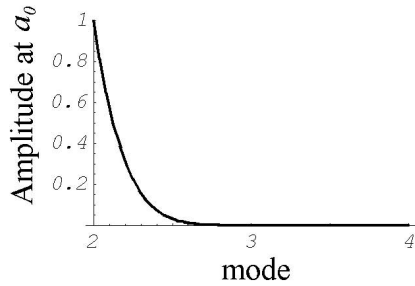


Figure 6: Amplitude of the inmost lamella (Normalized by the amplitude of the mode of  $m = 2$ ): Only the mode of  $m = 2$  reaches the axon

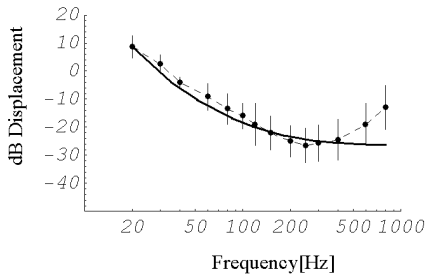


Figure 7: The tuning curve of Pacinian corpuscles: - - -: Experiment[18] —: Theory

with the experimental curve below the characteristic frequency can be confirmed.

In this way, the structure of the layered lamellae of Pacinian corpuscles can detect skin's equiboluminal deformation of the minimum order of  $m = 2$ .

### 3 Skin distortion in active touch

It is necessary for a derivation of a principle of tactile displays, besides the analysis of properties of mechanoreceptors, to clarify deformation of a skin in active touch.

From the analysis[20] of a contact and a relative motion between a skin and an object which has a Gaussian surface, it is shown that normal stress of  $p$  and shear stress of  $q$  to the skin surface at the positions of the projections are

$$q = s + \frac{\sigma}{\beta}p, \quad p = \frac{E}{\pi} \cdot \frac{\sigma}{\beta}, \quad (10)$$

which vibrate temporally with a stick-slip frequency of  $f_{ss}$  expressed as

$$f_{ss}^{-1} = \frac{2}{\omega_0} (\pi - \tan^{-1} R + R), \quad (11)$$

$$R = \frac{(\mu_s - \mu_c)P}{m\omega_0 U}, \quad (12)$$

$$\mu_s - \mu_c = \frac{\pi(s - s')\beta}{E\sigma}, \quad \omega_0 = \sqrt{\frac{k}{m}}, \quad (13)$$

where  $E_o, E_s$ : Young's ratio of the object and the skin, respectively!  $\nu_o, \nu_s$ : Poisson's ratio of the object and the skin!  $s, s'$ : static and kinetic shear strength of the skin,  $\sigma$ : standard deviation of the topography,  $\beta$ : mean radius of projections of the topography,  $P$ : a total normal pressure by the skin,  $U$ : a velocity of the motion,  $m, k$ : mass and elasticity of the skin. The relation between the parameters of an object and the stick-slip frequency, which is a key relation for displaying material quality in section 4, is drawn in Fig.8 with, for example,  $P = 1[\text{N}]$ ,  $m = 1[\text{g}]$ ,  $k = 500[\text{N/m}]$ ,  $U = 4[\text{cm/s}]$ .

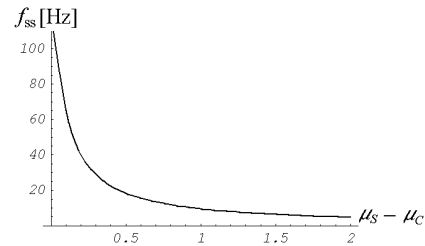


Figure 8: A relation between a parameter of  $\mu_s - \mu_c$  and a stick-slip frequency

Under these boundary conditions at the skin surface, let us consider deformation inside the skin. At the moment of the shift from the stick state to the slip state, the normal and the shear stresses begin to move suddenly on the skin surface. As a result, elastic waves are created inside the skin[21], which are dominant deformations because amplitudes are much greater than the other stationary deformation. Displacements inside the skin are drawn in Figs. 9 and 10 when the normal and shear stresses that vary with time as the Heaviside unit function are applied to the skin surface (We call these surface stresses 'the normal source' and 'the shear source').

The remarkable point is that the polarity of the S-wave's amplitudes in Fig.b), which are much larger than the P-wave's amplitude in Fig.a), turns over along the horizontal axis by the normal source (Fig.9b)) in contrast to the constant polarity by the shear source (Fig.10b)). As a result, the S-waves by many normal sources distributed over the skin surface are canceled as in Fig.11a), while the S-waves by the distributed shear sources become large due to a constructive interference as in Fig.11b). In this way, it is shown that primal surface stress, which creates dominant deformation inside the skin, is dispersed shear stress.

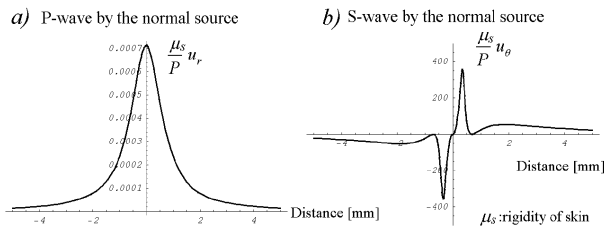


Figure 9: Amplitudes of P and S waves inside the skin when a normal source of  $P$  is applied to the skin surface: The horizontal axis is a distance along the skin surface from the point where the stress is applied

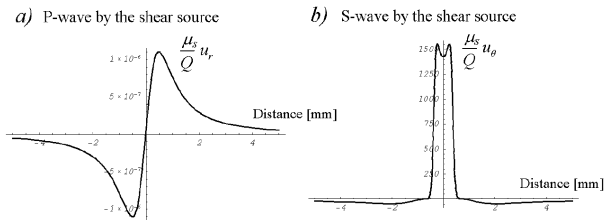


Figure 10: Amplitudes of P and S waves when a shear source of  $Q$  is applied to the skin surface

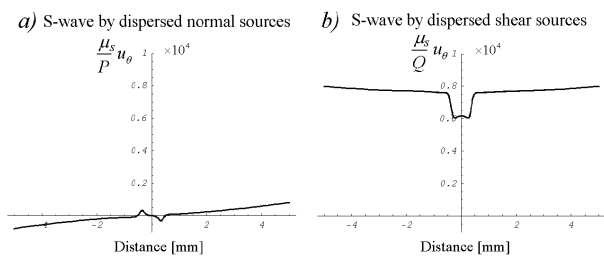


Figure 11: Amplitudes of S-waves by several sources dispersed at the intervals of 1[mm] on the finger surface: a) By normal sources b) By shear sources

1) Parameters of the object to be touched and the motion of an active touch:  $(E_0, \nu_0, \sigma, \beta) \times (P, U)$

2) Stress on the skin surface

$$\left\{ \begin{array}{l} \text{Dispersed sources of shear stress! } 'q = s + E/\pi \cdot (\sigma/\beta)^2 \\ \text{Stick-slip frequency! } 'f_{ss} = 1/T_{ss} \text{ in (11) } \sim (13) \end{array} \right.$$

3) Equivoluminal deformation inside the skin (Fig.11b))

4) Meissner and Pacinian corpuscles: Detection of the equivoluminal deformation (sec.2). The ratio of the contribution of both corpuscles is changed by  $f_{ss}$ .

Figure 12: A flow of tactile information

The analyses in sections 2 and 3 are summarized as a flow of tactile information as in Fig.12.

## 4 SAW tactile display

### 4.1 Shear sources method

From the above discussion, the prerequisites for tactile control, especially for stimulating RA mechanoreceptors, can be driven as follows:

- Sources of shear stress should be applied to the skin surface in order to create equivoluminal distortion detected by mechanoreceptors.
- The sources of shear stress can be spatially dispersed on the finger surface
- The sources of shear stress can be temporally modulated with a stick-slip frequency of  $f_{ss}$  determined by the parameters of the object to be displayed.

Though previous tactile displays have used varied actuators ([1][2][3][4] and so on), almost all stimulation is perpendicular to the skin surface with the exception of two methods. The first method, which controls the parallel force to the skin surface, uses ultrasonic vibrations [5]. A frictional force between a metal plate and a finger, which is a shear stress to the skin surface, can be controlled by a squeeze-film effect. The display succeeded in creating a sensation as if the surface were smooth by a stationary vibration, or as if a small projection were recreated on the surface by a momentary vibration. The second method, which is supposed to be equal to control shear stress to the skin, uses several phase-inverted perpendicular vibrations [7]. In geophysical exploration, two phase-inverted P-wave vibrators are used as a source of an S-wave [22]. The fact that two vertical vibrators driven out of phase create an S-wave can be confirmed by the spatial pattern of amplitudes in Fig.9b). The display can create a sensation as if a smooth surface, a sponge, or a pin moved on the skin.

However, because the relative motion between the skin and a real object has not been analyzed until now, it is unclear how to temporally modulate shear stress, and it is impossible to control a sensation of roughness systematically as if diameters of small projections on a rough surface changed continuously. We propose to use SAW to generate sources of shear stress that satisfy the above three prerequisites for tactile control.

### 4.2 Device

SAW has recently attracted attention for sources of driving force for linear motors [23], in addition to its practical application as a filter for telecommunication

equipment. We use SAW as sources of shear stress to a finger surface for tactile control.

The structure of the tactile display is shown schematically in Fig.13. In a LiNbO<sub>3</sub> Y-cut substrate whose size is 17[mm] × 63[mm] × 1[mm], SAW is generated by an alternative voltage to an interdigital transducer (IDT). The wavelength of SAW is about 265[μm] with the driving frequency of 15[MHz]. One of the prominent advantages of the display is the thinness of the substrate of 1[mm] for creating stimuli to the finger.

IDTs are placed at both ends of the substrate. According to the use of progressive waves or standing waves, it is decided to apply an alternative voltage to one side or both sides of the IDTs. For generating standing waves effectively, Open Metal Strip Array (OMSA) are set after IDTs as reflectors.

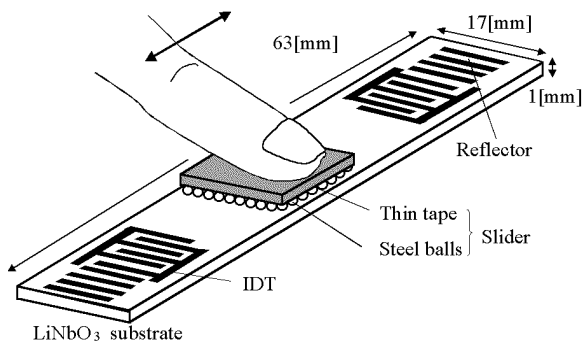


Figure 13: Schematic description of the SAW tactile display

In our tactile display, the substrate is explored with a 'slider' shown in Fig.16 in the last page. The slider has around 100 steel balls with a diameter of 800[μm] on a thin tape. The reasons to use a slider are as follows: 1) By pressing steel balls with the finger, a driving force can be effectively transmitted to the finger. 2) Steel balls can provide distributed points to which stress is applied on the finger surface, assuming that the tape is satisfactorily thin and soft.

### 4.3 Principle

The principle for generating sources of shear stress that are distributed spatially and modulated temporally is described in the following text.

When the substrate without SAW is explored by the finger with the slider, kinetic friction by the substrate is applied to the steel balls, thus creating sources of shear stress on the surface of the finger at the positions of all the steel balls distributed spatially (Fig.14 a)).

Now, by generating SAW, friction between the steel balls and the substrate is decreased compared to the

substrate without SAW for the following three reasons: 1) Decrease in contact time between the balls and the substrate; 2) A squeeze-film effect by the air that exists between the balls and the substrate; and 3) A parallel movement of the wave crest (only in using progressive waves). As a result, when either progressive or standing wave of SAW is generated in the substrate, shear stress to the skin becomes smaller (Fig.14 b)) than shear stress without SAW.

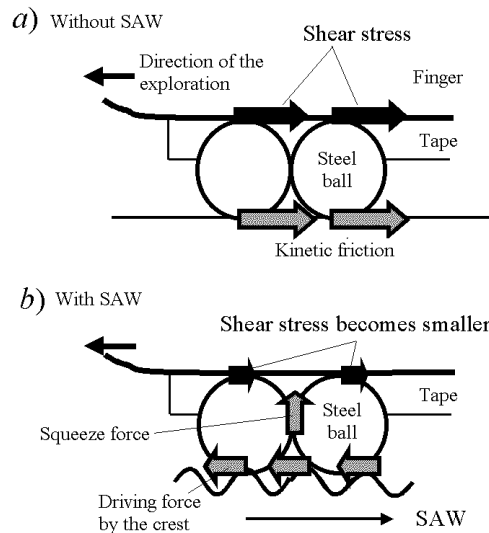


Figure 14: Generation of sources of shear stress that can be modulated temporally by burst SAW

Thus, by using a burst SAW, the sources of shear stress applied to the skin surface can be modulated with a burst frequency. The moment when the wave appears suddenly corresponds to the moment when the stick state changes into the slip state because the friction suddenly decreases. Therefore, the stick-slip frequency can be controlled virtually by changing the burst frequency. In this way, we obtain distributed sources of shear stress that are modulated with a stick-slip frequency determined by the solidity and the roughness of the object.

## 5 Experiments

In this section, we carry out experiments to control roughness of objects by changing the frequency of the modulation of the distributed sources of shear stress.

### 5.1 Generation of virtual stick-slip

Fig.15 shows an input signal of a burst wave to IDT and the resultant temporal change of friction.

The burst wave has a carrier frequency of 15[MHz] and a duty ratio of 40%. An input power is around 10[W] for standing waves and 100[W] for progressive waves. We use here standing waves.

In the curve of the measured data of friction between the slider and the substrate, a 89% decrease of friction from 1.56[N] to 1.4[N] under a normal pressure of 11.7[N] can be confirmed during generation of SAW. This is a virtual stick-slip vibration of friction. The burst frequency, denoted  $f_b$ , is a variable for controlling a tactile sensation in the next section.

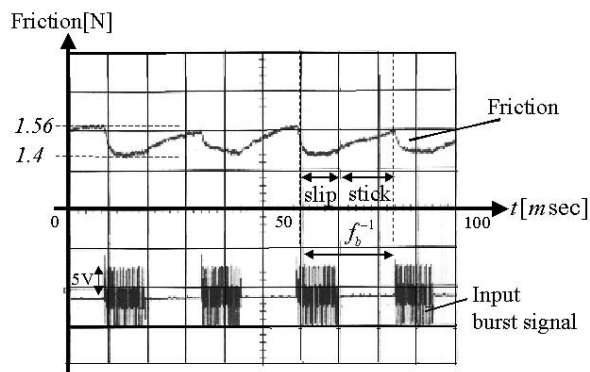


Figure 15: Experimental data of friction between the substrate and the slider. Friction is reduced by generating SAW. Thus, burst standing SAW can create virtual stick-slip vibration of friction.

## 5.2 Obtained tactile sensation

First of all, when the finger stops on the substrate, the vibration cannot be felt at all. However, exploring the substrate generates a sensation of roughness which is variable by the burst frequency of  $f_b$  as follows.

When  $f_b < 30$ [Hz], the surface feels bumpy as if there existed a row of small solid projections with an interval of a few [mm]. When  $30$ [Hz]  $< f_b < 100$ [Hz], the surface feels rough. With an increase of  $f_b$ , the roughness decreases as if the size and the intervals of the projections had become smaller. When  $f_b > 100$ [Hz], the surface feels smooth or slippery with low friction.

## 5.3 Evaluation

A Psychophysical experiment called Scheffé's method of pair comparison is carried out for an evaluation of the tactile display. Four real objects and four virtual roughness in the display are presented to three subjects. The real objects are sandpaper #60, #120, #240, and #320. The virtual roughness is presented by changing the burst frequency of 20[Hz], 40[Hz], 80[Hz], and 200[Hz]. A scale of the roughness of the real and the virtual surfaces is constructed by ranking the roughness of the pair presented. A virtual surface can be evaluated by a correlation between the ranking of the real and the virtual surfaces.

A composed scale of the roughness of the real and the virtual objects is provided as follows.

Real objects (Sandpapers)		Virtual objects (Display)	
The number	scale	$f_b$	scale
#60	-1.125	20[Hz]	-1.125
#120	-0.375	40[Hz]	-0.5
#240	0.375	80[Hz]	0.5
#320	1.125	200[Hz]	1.125

The correlation between the real and the virtual objects calculated from the above data is 0.98. The high value of the correlation is reasonable from a definite subjective difference between a bumpy surface with a frequency of 20[Hz] and a smooth one with a frequency of 200[Hz].

What characteristics of objects are presented in this SAW tactile display? The variable of  $f_b$  in the experiment corresponds in the real case to a stick-slip frequency of  $f_{ss}$ . As shown in Fig.8,  $f_{ss}$  increases when the  $\beta$ , which is the parameter of roughness, decreases. The experimental result that smoothness increases when  $f_b$  increases is justified by this fact. More precisely, as a parameter of the quality of the material, a stick-slip frequency determined by  $E\sigma/\beta$  can be represented in the SAW tactile display by a burst frequency of  $f_b$ .

## 6 Conclusion

In this paper, in order to obtain a principle for tactile displays, we first analyzed dynamic properties of mechanoreceptors and a skin. The results were as follows:

- Meissner corpuscles with coiled axons might easily detect shearing deformation of the skin due to the resultant stretches on the surface of the axons.
- Pacinian corpuscles might easily detect a minimum order equivoluminal distortion of the skin due to the rapid decay of the higher modes through the layered lamellae.
- In a contact and a relative motion between an object and a skin surface, stress generated at the skin surface, which creates dominant deformations inside the skin, is dispersed shear stress due to the constructive interference of distortion. The shear stress changes temporally with a stick-slip frequency determined by the parameters of solidity and roughness of the object.

From the above analyses, we obtained a prerequisite for tactile control that a tactile display should generate sources of shear stress that are spatially distributed and temporally modulated with a stick-slip

frequency. We proposed to use SAW for the generation of sources of shear stress that satisfy the prerequisite. A tactile display composed of a  $\text{LiNbO}_3$  substrate explored by a finger with a slider was produced. In the SAW tactile display, it was confirmed by psychophysical experiments that roughness could be controlled continuously by changing the burst frequency of SAW.

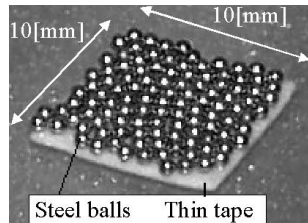


Figure 16: Slider

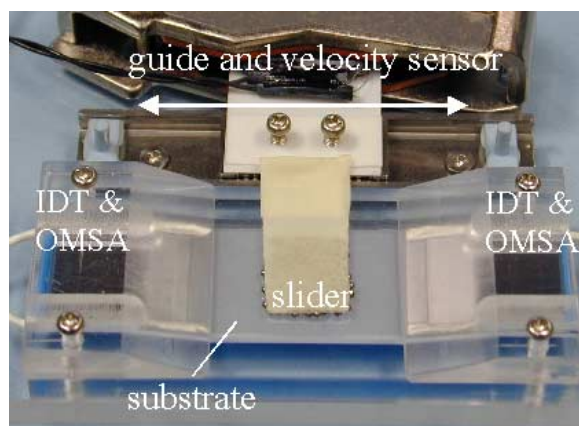


Figure 17: The SAW tactile display

## References

- [1] R.D.How e, et.al., Remote palpation Technology, IEEE Eng. in Medicine and Biology, Vol.14, No.3, pp. 318-323.
- [2] M. Akamatsu, et.al.: Multimodal Mouse: A Mouse-Type Device with T actile and Force Display, Presence, Vol.3, No.1, pp.73-80, 1994.
- [3] Y.Ikei, et.al.: Texture presentation by vibratory tactile display, Proc. IEEE VRAIS, IEEE, pp. 199-205(1996).
- [4] Sato.A, et.al.: Development of Non-Constrained Arm with T actile Feedback Device, Proc. IEEE ICAR, pp.334-338(1991).
- [5] T.Watanabe, et.al.: A Method for Controlling T actile Sensation of Surface Roughness Using Ultrasonic Vibration, Proc. IEEE ICRA, pp.1134-1139(1995).
- [6] R.S.Johansson et.al.: T actile Sensory Coding in the Glabrous Skin of the Human Hand, Trends in Neurosci., 6, pp.27-32, 1983.
- [7] N.Asamura, et.al.: A T actile Feeling Display Based on Selective Stimulation to Skin Receptors, Proc. IEEE VRAIS, pp.36-41(1998).
- [8] H.Kajimoto, et.al.: T actile Feeling Display Using Functional Electrical Stimulation, Proc. ICAT, pp.107-114(1999).
- [9] K.H.Andrew, et.al.: Morphology of Cutaneous Receptors, Handbook of Sensory Physiology, Vol.II, Springer Verlag, p.16(1973).
- [10] T.Tachibana, et.al.: Ultrastructural localization of calcium in mechanoreceptors of the oral mucosa, J. Neurocytol., 21, pp.745-753(1992).
- [11] F.Guharay, et.al.: Stretch-activated single ion channel currents in tissue-cultured embryonic chick skeletal muscle, J. Physiol., 352, pp.685-701(1984).
- [12] J.Zelena: Nerves and Mechanoreceptors, Chapman&Hall, p.230(1994).
- [13] W.Talbot, et.al.: The Sense of Flutter-Vibration, J. Neurophysiol., 31, pp.301-334(1967).
- [14] J.Bell, et.al.: The Structure and Function of Pacinian Corpuscles: A Review, Progress in Neurobiol., 42, pp.79-128(1994).
- [15] W.R.Loewenstein et.al.: Mechanical Transmission in a Pacinian Corpuscle. An Analysis and a Theory, J. Physiol., 182, pp.346-378(1966).
- [16] J.Bell and M.H.Holmes: Model of the Dynamics of Receptor Potential in a Mechanoreceptor, Mathematical Biosciences, 110, pp.139-174(1992).
- [17] S.J.Hubbard: A Study of Rapid Mechanical Events in a Mechanoreceptor, J. Physiol., 141, pp.198-218, 1958.
- [18] S.J.Bolanowski,Jr. et.al.: Intensity and Frequency Characteristics of Pacinian Corpuscles. I., J. Neurophysiol., 51, 4, pp.793-811(1984).
- [19] P.Nayak: Random process model of rough surfaces, J. lubrication tech., pp.398-407(1971).
- [20] T.Nara et.al.: An application of SAW to a Tactile Display in a Virtual Reality, Proc. IEEE Ultrasonics Symposium (to be printed).
- [21] C.C.Chao: Dynamical Response of an Elastic Half-Space to Tangential Surface Loadings, J. Applied Mechanics, 27, pp.559-567(1960).
- [22] H.A.K.Edelmann: SHOVER Shear-Wave Generator by Vibration Orthogonal to the Polarization, Geophysical Prospecting, 29, pp.541-549, 1981.
- [23] M.Takahashi, et.al.: Direct Frictional Driven Surface Acoustic Wave Motor, Proc. Transducers, pp.401-404, 1995.